Executive Summary

The purpose of this project was to develop a process for growing high-quality Indium Aluminum Nitride (InAlN) film on a Gallium Nitride (GaN) substrate using metal organic chemical vapor deposition (MOCVD). A GaN/AlGaN/AlN buffer structure was used to allow growth of the InAlN/GaN structure on a Si (111) substrate. Due to matching material properties of InAlN/GaN, this heterostructure has the potential to be used for High Electron Mobility Transistors (HEMTs) robust enough to operate in extreme high-temperature environments. InAlN films require precise temperature control (+/- ~5-10°C) as temperature is the most significant factor in determining the indium content in the finished film. Regarding quality, the only requirements were that the surface be (relatively) flat and smooth, and that the crystal quality be good enough that a measurable XRD signal could be detected from a ~30nm film. Throughout this experiment, figuring out how to control the growth temperature of InAlN comprised most of the time commitment. A total of nine InAlN films were grown at a variety of temperatures, most of which contained an overabundance of indium (in accordance with the XRD peaks) and had very rough surface topographies.

MOCVD of InAlN/GaN on Si Heterostructures for High-Temperature High-Electron-Mobility Transistors (HEMTs)

Thomas Heuser and Ricardo Peterson

SNF Mentor: Dr. Xiaoqing Xu - Industry Mentor: Dr. J Provine

Introduction:

The goal of this project was to develop a technique for producing high-quality indium aluminum nitride on gallium nitride (InAlN/GaN) high electron mobility transistors (HEMTs) designed for operation in corrosive, extreme high-temperature environments using metal organic chemical vapor deposition (MOCVD). Wide-bandgap semiconductor devices are of great interest for extreme environment operation, as they have the potential to withstand high temperatures, corrosive atmospheres, radiation-rich environments, each of which rapidly degrades the electrical behavior of low-bandgap materials.

A HEMT is a device architecture in which a heterojunction is formed between two spontaneously electrically polarized films. Making this structure causes energy bands to bend, forming a 2-dimensional quantum well to form near the interface that contains a dense sheet of electrons with extremely high carrier mobilities, known as the two-dimensional electron gas (2DEG). This can be seen in Fig. 1.

Currently, most wide-bandgap HEMT devices are based on aluminum gallium nitride (AlGaN)/GaN film stacks. Due to the

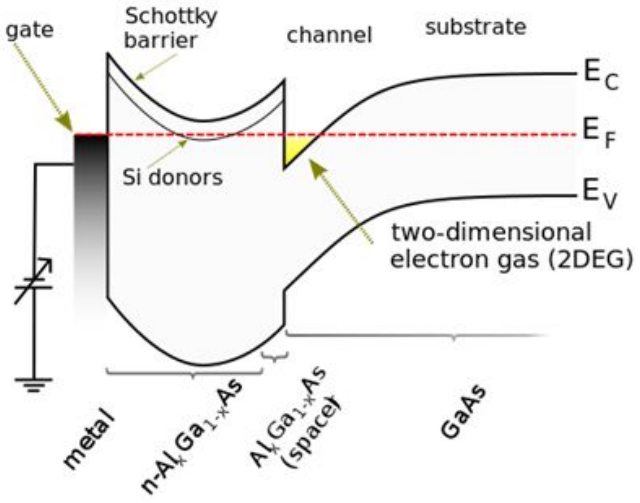

Figure 1.) Band Diagram of a High-Electron-Mobility Transistor

https://en.wikipedia.org/wiki/High-electron-mobility_transistor#/media/File:HEMT-band_structure_scheme-en.svg

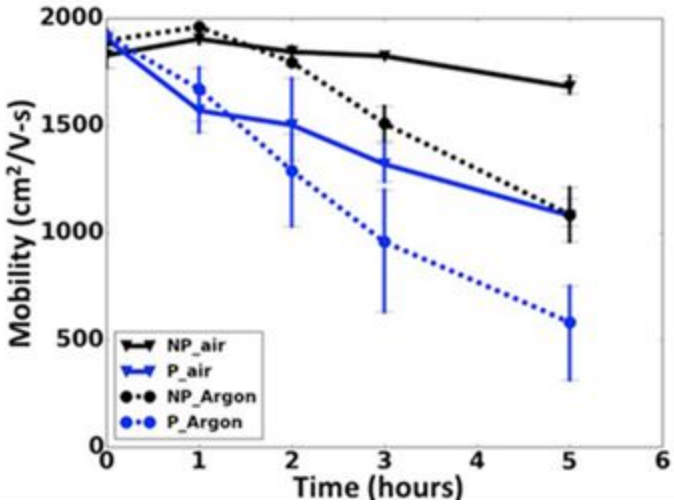

Figure 2.) AlGaN/GaN HEMT mobility degradation with time at 600C

Hou, M., Jain, S. R., So, H., Heuser, T. A., Xu, X., Suria, A. J., & Senesky, D. G. (2017). Degradation of 2DEG transport properties in GaN-capped AlGaN/GaN heterostructures at 600° C in oxidizing and inert environments. Journal of Applied Physics, 122(19), 195102.

low thickness of the AlGaN layer and the lattice mismatch between the two films, the AlGaN film is tensile strained, which significantly enhances the built-in electric field (i.e. piezoelectric polarization).

Unfortunately, the tensile strain of the AlGaN film has serious implications for high-temperature applications. Due to the differences in the coefficients of thermal expansion between AlGaN and GaN, it has been demonstrated that strain relaxation occurs, reducing the carrier mobilities significantly, as shown in Fig. 2. As this strain-relaxation behavior makes AlGaN/GaN devices unsuitable for high-temperature operation, another, related material belonging to the GaN-based HEMT family, InAlN/GaN, is used instead. At a specific indium concentration (~17-18%), InAlN becomes lattice-matched with GaN, thus lowering the concern for lattice relaxation at high temperatures. Moreover, the difference in spontaneous polarization coefficients between InAlN and GaN is significant enough to produce a 2DEG layer even without strain-induced piezoelectric polarization, thus making InAlN/GaN heterostructures a better candidate for HEMTs for high-temperature environments.

Over the course of this class, nine separate InAlN films were grown. Control of the true growth temperature posed the greatest challenge, which was the primary parameter used to modulate the desired InAlN properties. The surface quality of each film was determined using SEM, and the composition (in addition to crystallinity) was verified using XRD. Finally, in the last week, metal contacts were evaporated onto two separate growths, which were used to validate the existence of a 2DEG layer using Hall effect measurements.

Buffer Structure:

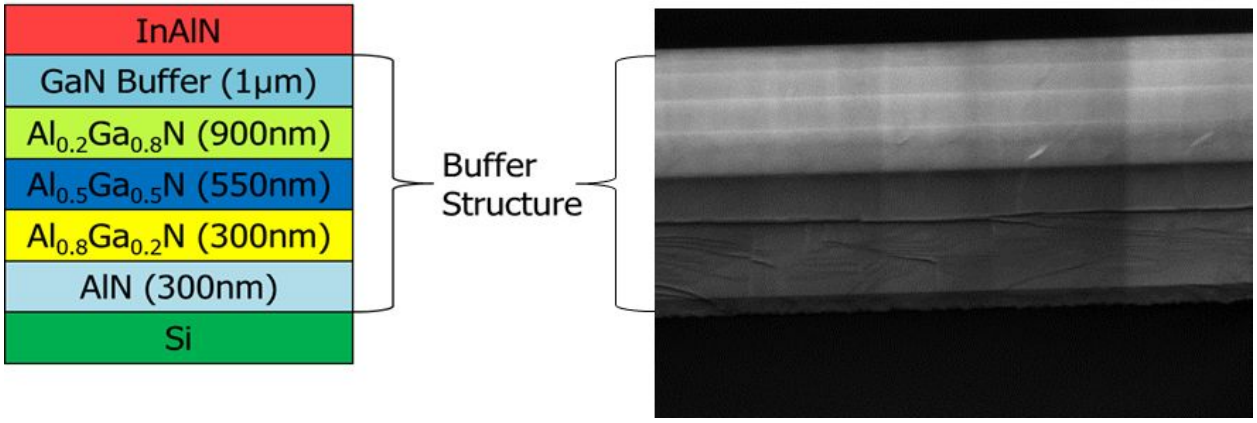

Figure 3.) Schematic and cross-sectional SEM of InAlN/GaN film stack

The use of silicon as a substrate provides a number of benefits (low cost, ease of integration with silicon CMOS, ability to release fabricated devices from substrate, etc.), but, as it is not lattice matched with GaN (~15% mismatch), a buffer structure is necessary. A full schematic of the buffer structure can be found in Fig. 3. The XRD of the buffer structure before InAlN growth can be found in Fig. 4. The first layer of the buffer is aluminum nitride (AlN) to serve as a nucleation layer. The next three layers are varying concentrations of aluminum gallium nitride (AlGaN), which serve two purposes: the first is to step the lattice constant from that of AlN to that of GaN, and the second is to engineer the strain such that the surface has no net strain at the beginning of the GaN growth. This structure was originally developed and validated for AlGaN/GaN on silicon structures outside of ENGR 241, but is equally applicable to growth of InAlN/GaN on silicon.

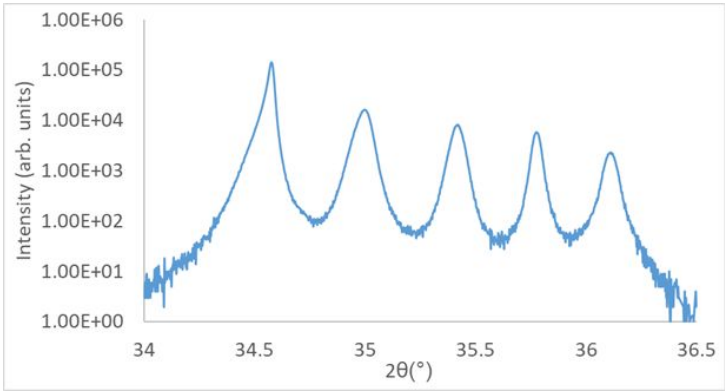

Figure 4.) XRD of bare buffer structure (no InAlN)

Fabrication:

The film stack was grown in the aix-ccs MOCVD in room 213XA in the Allen Extension Building. The recipes used in this project can be found in the users folder of the MOCVD (Anyone interested in growing InAlN/GaN should contact Dr. Xiaoqing Xu). The aix-ccs MOCVD is in the clean tool group, so before any growth can be done, substrates were subjected to a full RCA clean at the wbclean wetbenches. Substrates were (111) 4" silicon wafers, 700 μm thick instead of the standard 525 μm, because thicker substrates are less susceptible to bowing brought on by lattice-mismatched strain, thus producing a more uniform finished film. In order to reduce overall growth time and cost associated with growing the full buffer structure for each sample, it was grown on a single wafer that was then fractured to produce smaller growth template pieces, as shown in Figure 8. To facilitate Hall effect measurements, metal contacts were grown using a shadow mask and the AJA Evaporator located in ExFab room 155A in the Allen Building.

Figure 5.) aix-ccs MOCVD tool

Temperature Control:

Controlling the true temperature of the sample in the MOCVD chamber proved to be a challenging task. The susceptor used had three 2-inch wafer pockets, of which two were filled with dummy sapphire wafers. The process temperature, which is the temperature of the source, is acquired via a thermocouple. The temperature of the sample (i.e. true temperature), is acquired via pyrometry. The objective was to obtain a one-to-one mapping of the controllable temperature (process) to the sample temperature (true). This attempt is summarize in Figure 6. The red-colored text of

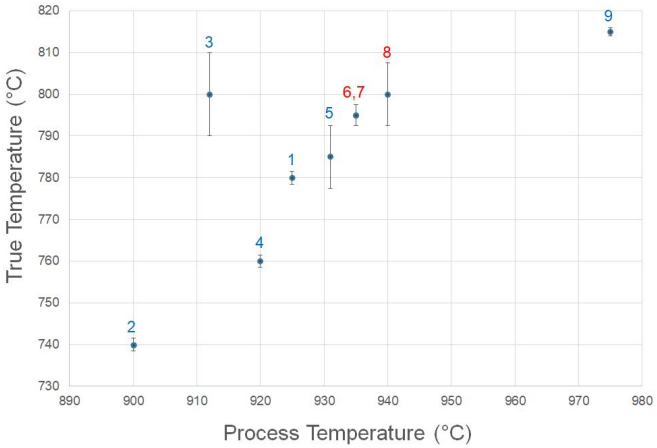

Figure 6.) aix-ccs True Temperature vs. Process Temperature for growth of InAlN on pieces.

samples 6, 7, and 8 represent erroneous temperature readings caused by pyrometer misalignment that were artificially corrected to sensible values.

To align the pyrometer, first place the sample into the desired pocket on the susceptor. If working with a small piece, try to center it in the pocket as much as possible. Close the reactor, and, in the control software, manually increase the susceptor rotation rate to 60 rpm (in increments of 20 rpm) to turn on the reflectivity monitor. Check the reflectivity monitor to ensure that the signal is centered on the template (and not overlapping an edge). Manually reduce the rotation rate (in increments of 20 rpm) to 0 rpm. If the growth template is not centered, open the reactor, reposition it, and re-check the alignment. Repeat this process as needed until the reflectivity monitor clearly shows the presence of a sample. Please note that alignment is only necessary for samples smaller than the diameter of the pocket. Samples that fit firmly into the pocket (e.g. full wafers) should not have any alignment issues.

Based on the pyrometer readings, it is suspected that the true growth temperature was a strong function of previous precursor emissions in the chamber. The basis of this assumption lies in the emissivity of the susceptor. Since the heat transfer mechanism from the heat source to the susceptor is primarily radiative, ambiguity in the emissivity constants fundamentally undermines any predetermined mapping of the True and Process temperatures. Thus, it is critical to ensure the replicability of the susceptor thermal properties before each growth.

This was attempted by growing a ~20nm GaN layer before the InAlN growth process. This decision was made for two reasons: (i) coating of Gallium precursors would ensure that the susceptor emissivity remains constant across different growths, and (ii) the growth of a thick GaN layer already precedes the InAlN layer during an entire InAlN/GaN growth; this is good practice for replicability assurance. Even with this, however, the true temperature can drift lower over the course of film growth. The process and true temperature statistics are shown in Figure 7. It is evident that samples 3 and 5 have the largest variance, which is attributed to the failed attempt to control the true temperature of sample.

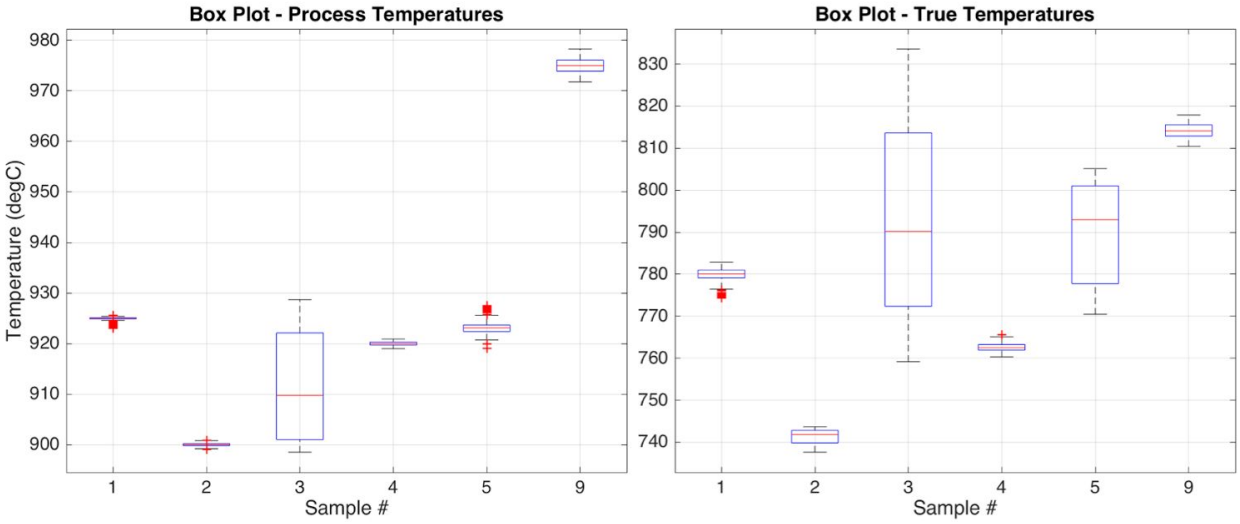

Figure 7.) Variation in Process Temperature (left) and True Temperature (right) for different growths

Results:

After film growth, the pieces were examined with surface and cross-sectional scanning electron microscopy in the Zeiss Sigma FESEM in the Beckman Center Cell Sciences Imaging Facility (CSIF) and the FEI XL30 Sirion SEM in the Stanford Nano Shared Facilities (SNSF). Afterwards, the X'Pert 1 X-Ray Diffractometer in the SNSF X-Ray Lab was used to take XRD sample from each sample, which allowed for determination of composition through the positioning of the InAlN peak, as well provided qualitative information regarding the crystalline quality of the film. When the InAlN is not lattice-matched to GaN, the crystal quality of the film is significantly reduced, and the XRD signal it produces is much lower.

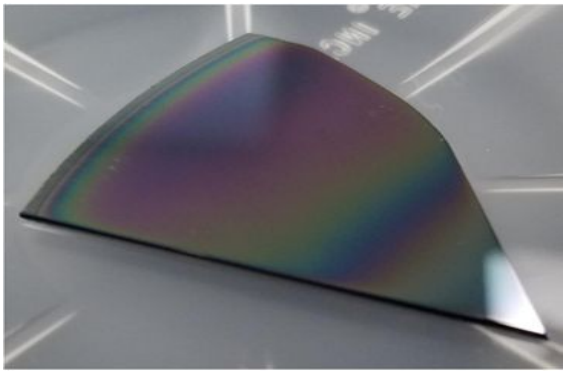

Figure 8.) Sample with ~200 nm as-grown InAlN layer

At the beginning of the experiment, before the sample compositions were in the correct range, thicker (~200 nm) InAlN films were grown to ensure that the XRD signal would be strong enough to be visible over the background produced by the buffer structure. As the composition approached the correct value over the course of the

experiment, InAlN thickness was lowered to ~30nm. The first three samples growths had very rough, uneven surface morphologies, the origins of which are undetermined, although lattice mismatch may be an explanation. Additionally, the first samples were the thickest of them all, ranging from 200-250nm. Interestingly, as the InAlN layer thickness decreased to ~150nm, as was the case for samples 4 through 6, 'barnacle-like' morphologies were observed, as shown in Figure 10.) (bottom-left). In particular, the SEMs of sample 5 hinted at an underlying reality. First, sparse flat regions can be seen, which is unlike the extremely rough surface of previous samples. Second, the 90° cross section of sample 5 exhibits grooves that terminate about ~50nm from the InAlN/GaN interface. This indicated that these morphologies may begin to form once the layer is thick enough.

Even after reaching the desired indium concentration, the surface morphology of the final films is not perfect. As seen in Fig. 10, sample 9 contains pinholes and has a patchy texture. We theorize that this may result from an imperfect starting surface caused by partial decomposition of the buffer during the pre-growth high-temperature bake step. If this is the case, growing the entire stack in one run, rather than growing the buffer first and InAlN later, may prevent this, as the buffer structure would never experience temperatures extreme enough to cause decomposition.

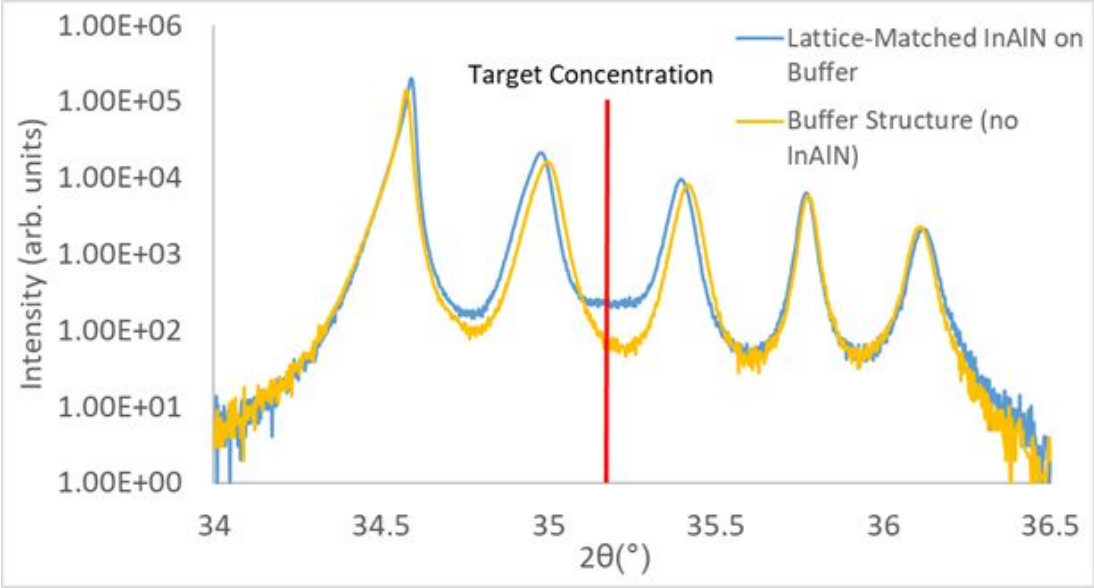

Figure 9.) XRD spectra of InAlN/GaN (sample 9) structure with correct InAlN composition vs. spectra of bare buffer structure.

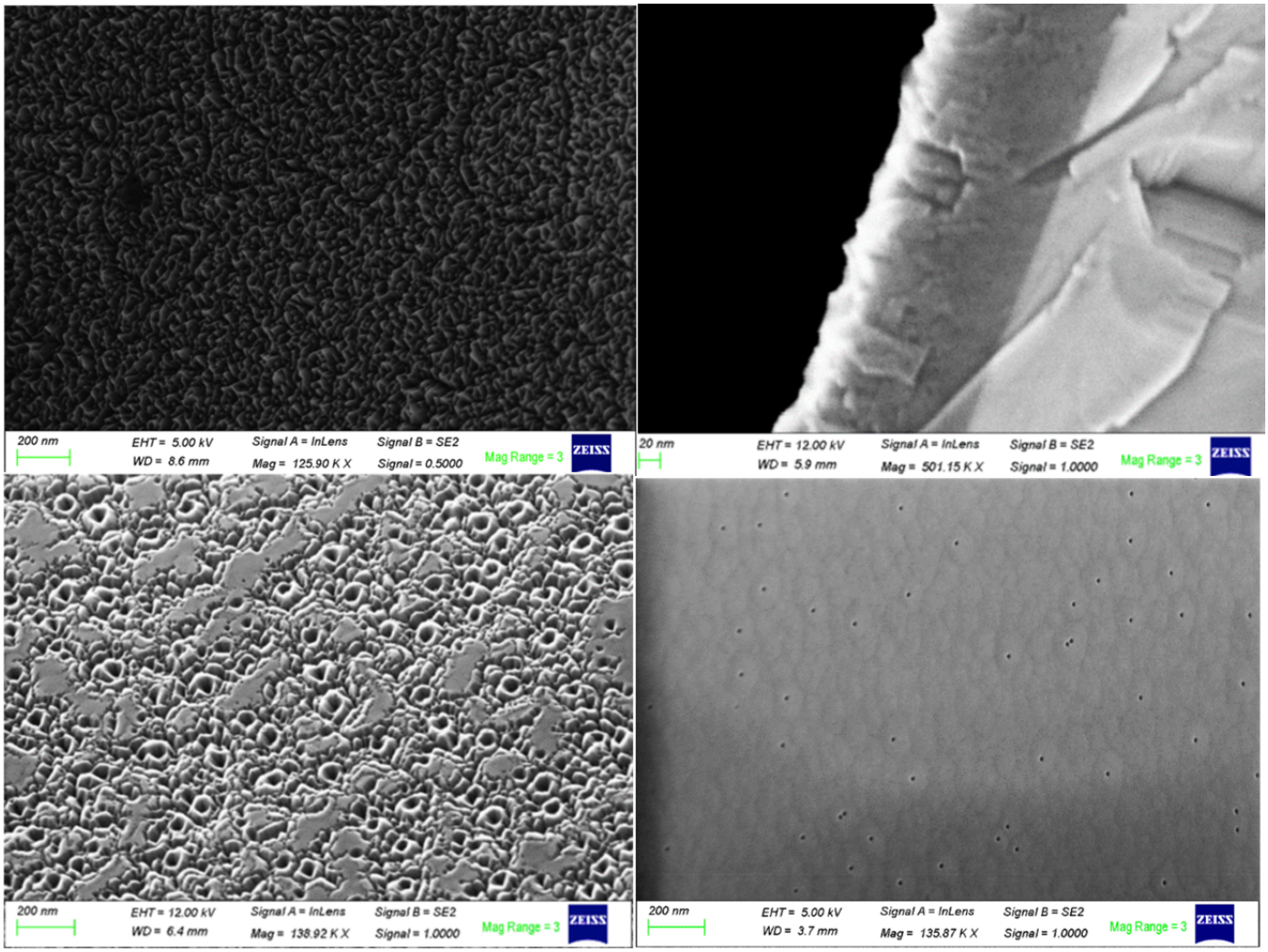

Figure 10.) Sample 1 surface (top-left), Sample 5 surface (bottom-left), Sample 5 cross section (top-right), Sample 9 surface (bottom-right).

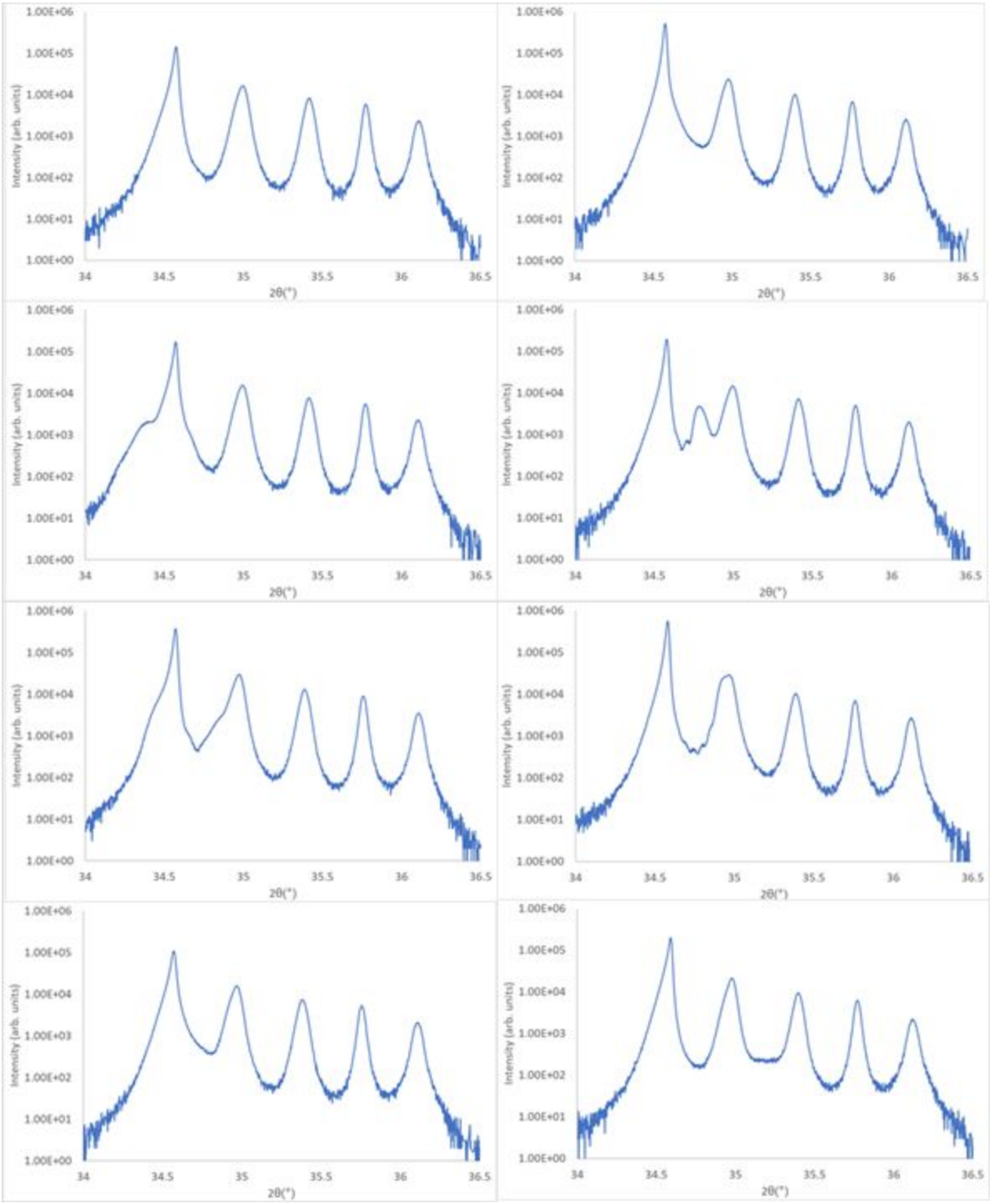

Figure 11.) XRD spectra of samples 1-4 (left) and 5, 7-9 (right)

Hall Effect Measurements:

Figure 12.) InAlN/GaN Hall effect test structure

Although the objectives of this project was primarily concerned with MOCVD growth of InAlN-on-GaN, a HEMT structure is not possible unless a 2DEG exists along heterostructure interface. Therefore, confirming the existence of a conducting channel was the obvious follow-up. Upon the growth of the ultra-thin InAlN film (sample 9), Hall Effect measurements were taken. The AJA e-beam evaporator and a shadow mask were used to evaporate a Ti/Al/Pt/Au metal contact at 20/100/40/80 nm thicknesses. It is important to note that this particular metal stack was developed for AlGaN/GaN HEMTs. Due to time constraints, however, experimenting on metal stacks for InAlN/GaN HEMTs was not possible. Looking forward, optimization of the ohmic contacts will be a necessary step.

The extracted mobility values are shown in the table below. Contacts were grown on samples 6 and 9, which have the ultra-thin InAlN films needed for 2DEG layers to form. It was expected that, due to the electrically active defects in the InAlN layer, conduction from the 2DEG to the metal contacts would be sufficient to extract mobilities. According to the van de Pauw measurements, a pre rapid-thermal-anneal (RTA) mobility of 206 cm^2/V*s was measured for sample 6, while sample 7 exhibited an open circuit, presumably due to poor contact quality. Mysteriously, post-RTA significantly degraded the mobilities to 20 cm^2/V*s for both samples. This observation may be explained as follows: during the annealing phase, metal atoms exhibit lateral and transverse diffusion, which induces significant carrier scattering. In addition, the surface area of the metal/InAlN contact is unnecessarily large, which only exacerbates this issue. Therefore, in conjunction to optimizing metal stacks for InAlN, patterning of smaller contact areas will be necessary.

It is necessary to note that the objective here was to confirm the existence of a 2DEG, which is highly likely based off of the extracted mobilities of the Hall measurements. However, the subject of characterizing and optimizing HEMT electrical behavior merits an entire project of its own.

Sample #	Growth Temperature (°C)	% Indium	InAlN Thickness (nm)	XRD (2θ)	Mobility (cm^2/V s) Pre/Post RTA
6	795	22	27	34.9	206 / 20.5
9	815	18	~25	35.2	-- / 20.5

Figure 13.) InAlN/GaN Preliminary Hall effect results

Acknowledgements:

We would like to thank our SNF mentor, Dr. Xiaoqing Xu, and our industry mentor, Dr. J Provine for their guidance and help on this project. Additionally, we would like to thank the staff of SNF, SNSF, and CSIF for maintaining the tools we used during this project, and Professor Jonathan Fan for teaching the course and providing useful feedback to project updates.

References:

[1] J. Xie, X. Ni, M. Wu, J. H. Leach, Ü. Özgür, and H. Morkç, "High electron mobility in nearly lattice-matched AlInNAlNGaN heterostructure field effect transistors," *Appl. Phys. Lett.*, vol. 91, no. 13, 2007.
[2] R. Butté, J. F. Carlin, E. Feltin, M. Gonschorek, S. Nicolay, G. Christmann, D. Simeonov, A. Castiglia, J. Dorsaz, H. J. Buehlmann, S. Christopoulos, G. Baldassarri Höger Von Högersthal, A. J. D. Grundy, M. Mosca, C. Pinquier, M. A. Py, F. Demangeot, J. Frandon, P. G. Lagoudakis, J. J. Baumberg, and N. Grandjean, "Current status of AlInN layers lattice-matched to GaN for photonics and electronics," *J. Phys. D. Appl. Phys.*, vol. 40, no. 20, pp. 6328–6344, 2007.
[3] K. Jeganathan, M. Shimizu, H. Okumura, Y. Yano, and N. Akutsu, "Lattice-matched InAlN/GaN two-dimensional electron gas with high mobility and sheet carrier density by plasma-assisted molecular beam epitaxy," *J. Cryst. Growth*, vol. 304, no. 2, pp. 342–345, 2007.
[4] J. F. Carlin and M. Ilegems, "High-quality AlInN for high index contrast Bragg mirrors lattice matched to GaN," *Appl. Phys. Lett.*, vol. 83, no. 4, pp. 668–670, 2003.
[5] M. Hou, S. R. Jain, H. So, T. A. Heuser, and X. Xu, "Degradation of 2DEG transport properties in GaN-capped AlGaN/GaN heterostructures at 600 °C in oxidizing and inert environments," vol. 195102, 2017.